NJC

Accepted Manuscript

This is an *Accepted Manuscript*, which has been through the Royal Society of Chemistry peer review process and has been accepted for publication.

Accepted Manuscripts are published online shortly after acceptance, before technical editing, formatting and proof reading. Using this free service, authors can make their results available to the community, in citable form, before we publish the edited article. We will replace this *Accepted Manuscript* with the edited and formatted *Advance Article* as soon as it is available.

You can find more information about *Accepted Manuscripts* in the Information for Authors.

Please note that technical editing may introduce minor changes to the text and/or graphics, which may alter content. The journal's standard Terms & Conditions and the Ethical guidelines still apply. In no event shall the Royal Society of Chemistry be held responsible for any errors or omissions in this *Accepted Manuscript* or any consequences arising from the use of any information it contains.

ROYAL SOCIETY OF CHEMISTRY

www.rsc.org/njc

Journal Name

ARTICLE

Phase transition, morphological transformation and highly enhanced luminescence properties of YOF:Eu^{3+} crystals by Gd^{3+} doping

Received 00th January 20xx,
Accepted 00th January 20xx

DOI: 10.1039/x0xx00000x

www.rsc.org/

Ruiqing Li,[a] Nannan Zhang,[a] Linlin Li,[a] Yimai Liang,[a] Yali Liu,[a] and Shucai Gan*[a]

A series of undoped and Eu^{3+} doped YOF and $Y_{1-x}Gd_xOF$ (x = 0–0.7) crystals were prepared via a urea based homogeneous precipitation method followed by a heat treatment process. After doping Gd^{3+}, we first observed the crystal phase transition, morphology transformation, and greatly enhanced luminescence properties of YOF crystals. The results reveal that the Gd^{3+} addition can promote the phase transition from the hexagonal phase to the rhombohedral phase and the morphology transformation from spheres, though the mixture of rods and spheres, to spheres. The luminescence properties of Eu^{3+} doped YOF phosphors were investigated upon UV excitation and the quenching concentration of Eu^{3+} was found to be 10 mol%. More importantly, luminescence intensity after doping a certain amount of Gd^{3+} increased by 31 times than that of the Gd^{3+} free sample, which may due to the modification of crystal field and crystal phase of YOF, providing an effective way to gain numerous Gd^{3+} doped luminescence materials. These result shows that the Gd^{3+} doped red phosphors have potential applications in white light emitting diodes.

1. Introduction

In recent years, the lanthanide ions (Ln^{3+}) doped luminescent materials have attracted extensive attention due to their potential applications in displays, white light emitting diodes (WLEDs), lasers, medical diagnosis, and bio-labels.[1–6] And it is generally accepted that controlling the phase structure, morphology, and dimensionality of phosphors are very important due to the correlation between these parameters and optical properties. Therefore, many efforts have already been devoted to exploring synthetic methods for preparing these kinds of luminescent materials.[7–10] The use of morphology-control agents is an efficient strategy to control the size and shape, in which the functional groups of agents can preferentially adsorb on the crystal facet and then modulate the kinetics of crystal growth.[11,12] However, the obtained samples always suffer from the surface contamination due to the residual organic surfactants, which would affect the physical and chemical properties of final products.[13,14] Thus, it is still a challenge to establish a green, facile, and economic synthetic strategy for the synthesis of the high quality products with easy control over phase, and morphology.

At present, great endeavors are focused on increasing the luminescent intensity of phosphors. In general, there are several methods on enhancing luminescence, such as core–shell, and energy transfer processes.[15–17] Besides, impurity doping, is recently found to have significant influence on the nucleation and growth of many phosphors, and also provides an approach to modify the crystal phase, morphology, and electronic configuration of materials. For example, wang *et al.* obtained the conversion of CeO_2 nanopolyhedra into nanospheres by Ti^{4+} doping and You *et al.* reported rational tunability of the morphologies of GdF_3 by Ba^{2+} doping.[18,19] It was also found that lanthanide and some other metal ions doping could enhance luminescence intensity of the samples.[20–22] Lanthanide oxyfluorides (LnOF) have attracted extensive interest for applications in up-conversion (UC) and down-conversion (DC) luminescence due to the high ionicity, low phonon energy, better chemical and thermal stability compared with those of the fluorides and oxides.[23–25] Among them, YOF crystals with various morphologies have been successfully prepared by several methods such as thermolysis method, sol-gel method, hydrothermal method, and coprecipitation method.[26–29] Moreover, the Gd^{3+} based materials have been used as a contrast agent in magnetic resonance imaging (MRI) for medical diagnosis and a marker in bioprobes.[30,31] As far as we know, there is no systematic study on the phase structure, morphology, and photoluminescence (PL) improvement of YOF by introducing Gd^{3+} ions.

In this study, we synthesized a series of undoped and Eu^{3+}-doped $Y_{1-x}Gd_xOF$ crystals via a precipitation method followed by a heat-treatment process. The effect of Gd^{3+} doping on phase structure, and morphology of YOF has been investigated in detail. Moreover, the PL properties of YOF: Eu^{3+} phosphors have been discussed. For the optimal Eu^{3+} content (0.1 mmol in this study), the Gd^{3+} doping prominently enhanced red emission of Eu^{3+} for the as-prepared samples.

2. Experimental section

2.1 Materials

[a] *College of Chemistry, Jilin University, Changchun 130026, PR China*
E-mail: gansc@jlu.edu.cn

†Electronic Supplementary Information (ESI) available: XRD pattern of $Y_{0.2}Gd_{0.8}OF$ sample. XRD patterns of $Y_{0.9-x}Gd_xOF$:0.1Eu samples. The calculated lattice parameters of $Y_{0.9-x}Gd_xOF$ with different Gd^{3+} concentration. The CIE chromaticity coordinates of Gd^{3+} doped YOF:0.1Eu samples. See DOI:10.1039/x0xx00000x

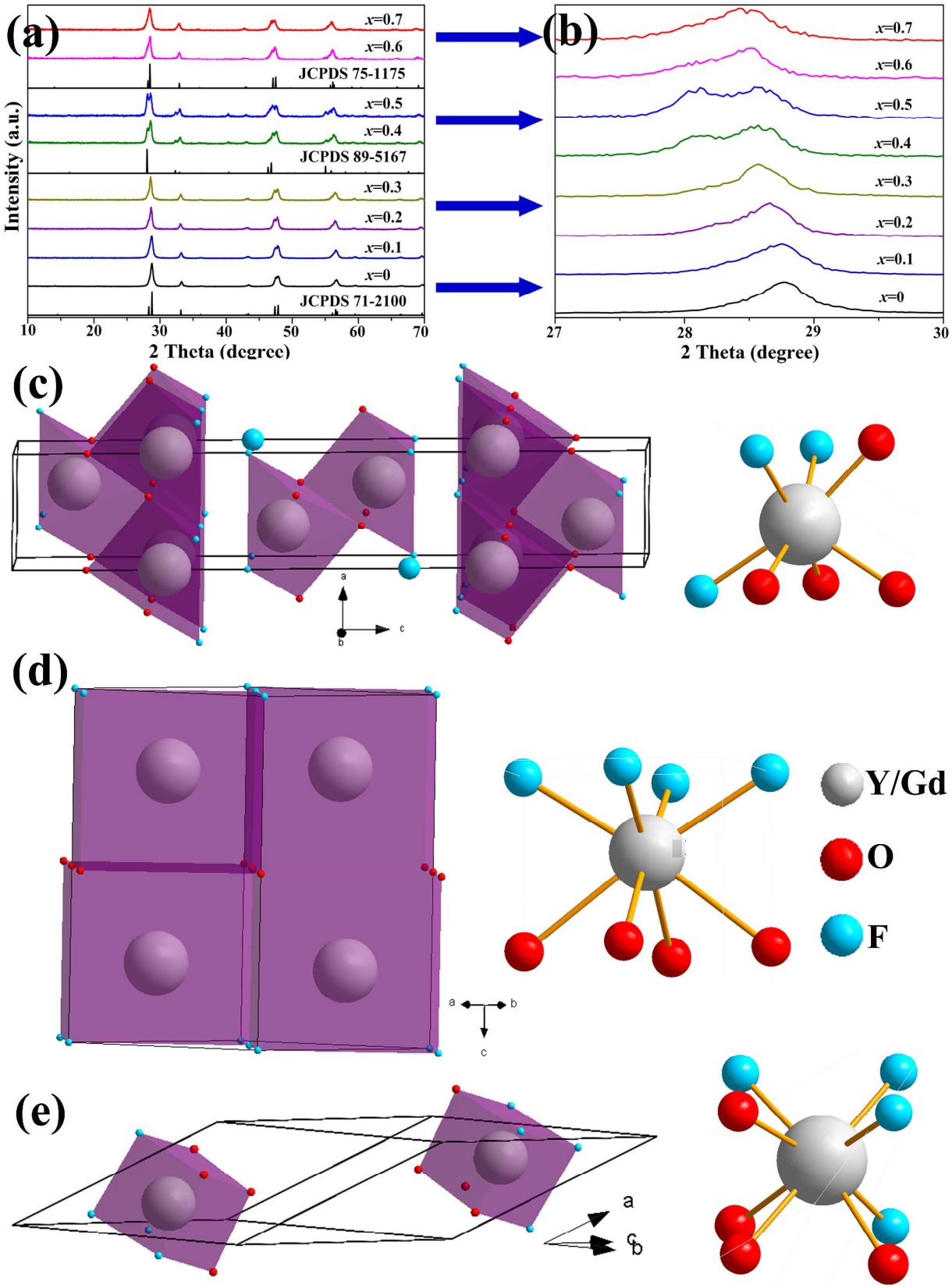

Fig.1 XRD patterns of $Y_{1-x}Gd_xOF$ (x = 0, 0.1, 0.2, 0.3, 0.4, 0.5, 0.6, and 0.7) samples (a); the zoom-in patterns of Fig. 1(a) in the range of 27–30° (b); Schemes of the hexagonal, tetragonal, and rhombohedral phase YOF structures (c), (d), and (e), respectively.

Rare earth oxides Ln_2O_3 (Ln = Y, Gd, and Eu, 99.99%) were supplied from Science and Technology Parent Company of Changchun Institute of Applied Chemistry. Other chemicals were purchased from Beijing Chemical Company. $Ln(NO_3)_3$ solution were prepared by dissolving the corresponding Ln_2O_3 in dilute HNO_3 solution at elevated temperature.

2.2. Synthesis

In a typical procedure 1 mmol $Y(NO_3)_3$ was added to 100 mL aqueous solution containing 3g urea and 0.25 mmol of $NaBF_4$ at room temperature. Then, dilute $NH_3 \cdot H_2O$ was introduced rapidly into the vigorously stirred solution until pH = 6 and then the beaker was wrapped with polyethylene film. After magnetic stirring for 30 min, the mixture was heated to 90 °C for 3 h in the water bath. The resulting white precipitates were collected by centrifugation, washed several times with deionized water and ethanol, and finally dried at 70 °C in air for 12 h. The final YOF sample was obtained by a heat treatment of precursors at 500 °C for 3 h in air.

A similar process was employed for preparing other sample except for a stoichiometric amount of $Eu(NO_3)_3$ and $Gd(NO_3)_3$ instead of $Y(NO_3)_3$ in the initial solution.

2.3 Characterization

The products were examined by powder X-ray diffraction (XRD) performed on a Rigaku D/max-II B X-ray diffractometer at a scanning rate of 3.5°/min in the 2θ range from 10° to 70°, with graphite-monochromatic Cu Ka radiation (λ = 0.15406 nm). The morphologies of the as-prepared crystals were investigated by means of a scanning electron microscope (SEM, S-4800, Hitachi). The PL excitation and emission spectra were recorded using a Hitachi F-7000 spectrophotometer equipped with a 150 W xenon lamp as the excitation source. All measurements were performed at ambient temperature.

3. Result and discussion

3.1. Crystalline phase and morphology of the samples

Fig. 1 shows the XRD patterns of the YOF samples with different Gd^{3+} contents. The XRD of undoped sample is identified as hexagonal YOF (JCPDS 71–2100). No extra impurity diffraction peaks were observed, indicating the formation of pure hexagonal phase structure. With the addition of 0.1–0.3 mmol Gd^{3+} ions, the phase of the samples is still maintained. By increasing the Gd^{3+} ions to 0.4–0.5 mmol, the tetragonal phase and rhombohedral phase of YOF coexist. Further increasing Gd^{3+} ions content up to 0.6–0.7 mmol, the samples are all indexed to rhombohedral phase of YOF (JCPDS 75–1175). When the Gd^{3+} ions concentration reach reached 0.8 mmol, the product turns out to be hexagonal GdOF (Fig. S1 (ESI)). In addition, from Fig. 1b, the enlarged area of the main diffraction peak shows that the diffraction peak shifts towards lower angles with the increase of Gd^{3+}/Y^{3+} ratio due to larger Gd^{3+} (1.053 Å) ions substituting the Y^{3+} (1.019Å) ions, which may result in the expansion of unit cell volume in the host lattice.[32,33] Fig. 1c, d, and e depict the unit cell structure of hexagonal, tetragonal, and rhombohedral phase YOF and the coordination environment of the Y^{3+} ions. In three kinds of hosts, there all have one kind of cation sites. The Y^{3+} cations are coordinated by four O^{2-} and three F^- in the hexagonal YOF, while the Y^{3+} cations are coordinated by four O^{2-} and four F^- for the tetragonal and rhombohedral YOF.

Fig. 2a−h show the SEM images for YOF particles doped with various Gd^{3+} concentration. As shown in Fig. 2a, the obtained YOF sample without doping Gd^{3+} ions is composed of numerous spheres

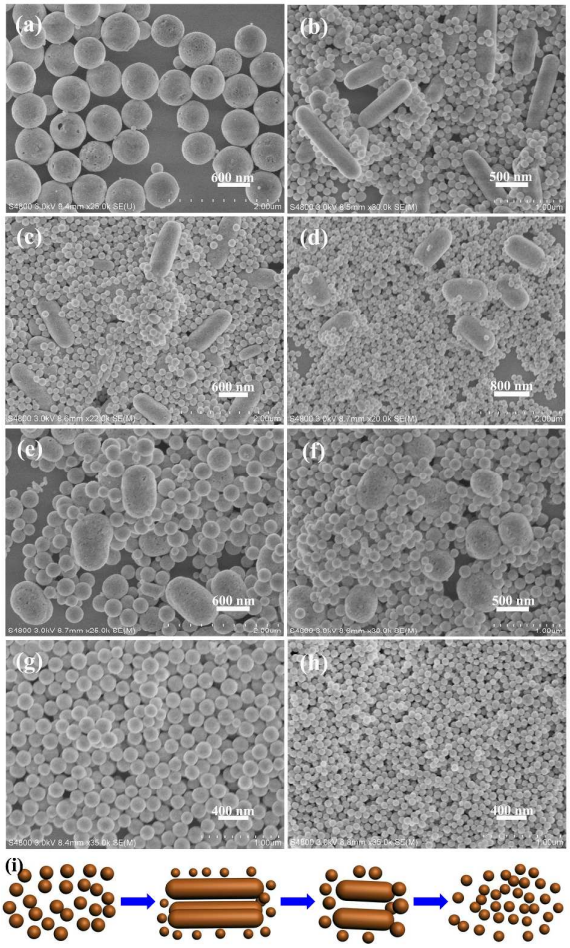

Fig.2 SEM images of $Y_{1-x}Gd_xOF$ with (a) x = 0, (b) x = 0.1, (c) x = 0.2, (d) x = 0.3, (e) x = 0.4, (f) x = 0.5, (g) x = 0.6, (h) x = 0.7. Schematic illustration of the formation process of YOF submicro spheres (i).

with a uniform size of 740 nm in diameter and the surfaces are rough. With the addition of 0.1 mmol, the as-prepared YOF product consists of a great number of monodispersed spheres and rods with a relative uniform size of 1.2 μm in length and 320 nm in diameter, and the aspect ratio of the product is about 4 (Fig. 2b). With increasing Gd^{3+} doping content from 0.1 to 0.2, the as-obtained YOF product exhibits similar morphology (Fig. 2c). The respective average length and diameter of the rods are about 1.15 μm and 460 nm, respectively, and the aspect ratio is about 2.5. By increasing the Gd^{3+} ions to 0.3, and 0.4 mmol, the aspect ratios of length and diameter of the rods decrease to 1.9, and 1.6, respectively (Fig. 2d and e). Further increasing the amount of Gd^{3+} up to 0.5 mmol, the as-obtained YOF product comprises of spheres with diameter of about 379 nm and 540 nm (Fig. 2f). When the Gd^{3+} concentration reached 0.6 and 0.7 mmol, the YOF products become highly uniform spheres (Fig. 2g and h). Therefore, the YOF with controlled shape and size can be achieved by only adjusting the doped Gd^{3+} contents. The morphology evolution of the samples upon increasing doping concentration may be attributed to the strong effect of Gd^{3+} ions on the crystal growth rate through surface charge modification, which is similar to previous reports that the La^{3+}, Mo^{3+} or Mn^{2+} ions doped in the crystals.[33–35] On the basis of the above experimental results and analysis, a schematic illustration for the formation of YOF product is presented in Fig. 2i.

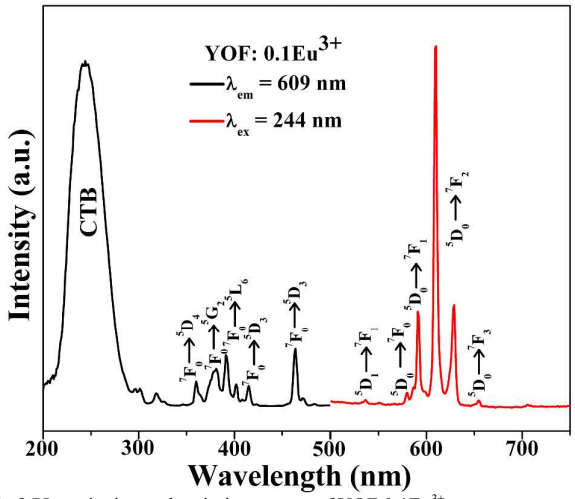

Fig.3 PL excitation and emission spectra of YOF:0.1Eu^{3+}.

3.2 Luminescent properties

Eu^{3+} ion is a well-known red-emitting activator in commercial phosphors because the emission of Eu^{3+} ion usually consists of line transitions in the red region due to the $^5D_0 \rightarrow {}^7F_J$ (J = 1, 2, 3, 4, 5 and 6) transitions.[36] Hence, in our experiment, the Eu^{3+} ion was selected as the doping ion to investigate the PL properties of the samples. Fig. 3 presents the PL excitation and emission spectra of the as-prepared YOF: Eu^{3+} spheres. The excitation spectrum monitored with 609 nm consists of a strong broad excitation bands from 200–290 nm with a maximum at 244 nm, which should be attributed to the charge transfer band (CTB) between O^{2-} and Eu^{3+}. In the longer wavelength region (350–500 nm), the weak peaks are intraconfigurational 4f–4f transition of Eu^{3+} at about 360 nm ($^7F_0 \rightarrow {}^5D_4$), 380 nm ($^7F_0 \rightarrow {}^5G_2$), 391 nm ($^7F_0 \rightarrow {}^5L_6$), 415 nm ($^7F_0 \rightarrow {}^5D_3$), and 465 nm ($^7F_0 \rightarrow {}^5D_2$). The emission spectrum is obtained under 244 nm excitation and displays two groups of PL bands corresponding to the $^5D_1 \rightarrow {}^7F_1$ and $^5D_0 \rightarrow {}^7F_J$ (J = 0, 1, 2, 3) transitions.[37] In case of Eu^{3+}, the $^5D_1 \rightarrow {}^7F_1$ emission transition is not main and the $^5D_0 \rightarrow {}^7F_{0,1,2,3}$ transitions with peak maximum at 580, 591, 609, 628, and 654 nm, respectively, are noteworthy. Generally, if Eu^{3+} ions are occupied in a site with inversion symmetry, the $^5D_0 \rightarrow {}^7F_1$ magnetic dipole transition is the strongest, while in a site without inversion symmetry, the $^5D_0 \rightarrow {}^7F_2$ electric dipole transition is domination. In the YOF:Eu^{3+} system, we can use the $I(^5D_0 \rightarrow {}^7F_2)/I(^5D_0 \rightarrow {}^7F_1)$ emission intensity ratio as a measure of the site symmetry of Eu^{3+}. And the intensity of red $^5D_0 \rightarrow {}^7F_2$ transition of Eu^{3+} at 609 nm is about 3.4 times stronger than that of $^5D_0 \rightarrow {}^7F_1$, which significantly indicates that the Eu^{3+} ions are located at a center of asymmetry in the crystal lattice.[38,39] The transition $^5D_0 \rightarrow {}^7F_2$ is much stronger than the transition $^5D_0 \rightarrow {}^7F_1$, which is favorable to improve the color purity of red phosphor.

To investigate the effect of concentration on the luminescence properties of samples, a series of YOF:$x$$Eu^{3+}$ (x = 0.01–0.12) were synthesized. Fig. 4a depicts the emission spectra of the phosphors with different Eu^{3+} contents under the 244 nm irradiation. With the increase of Eu^{3+} content, the luminescence intensity of phosphor first increases gradually to a maximum at x = 0.1 and then decreases due to the concentration quenching of the Eu^{3+} ions. Fig. 4b shows the variation of emission intensity as a function of doped Eu^{3+} content.

According to Dexter's energy transfer theory, concentration quenching is mainly caused by the non-radiative energy migration

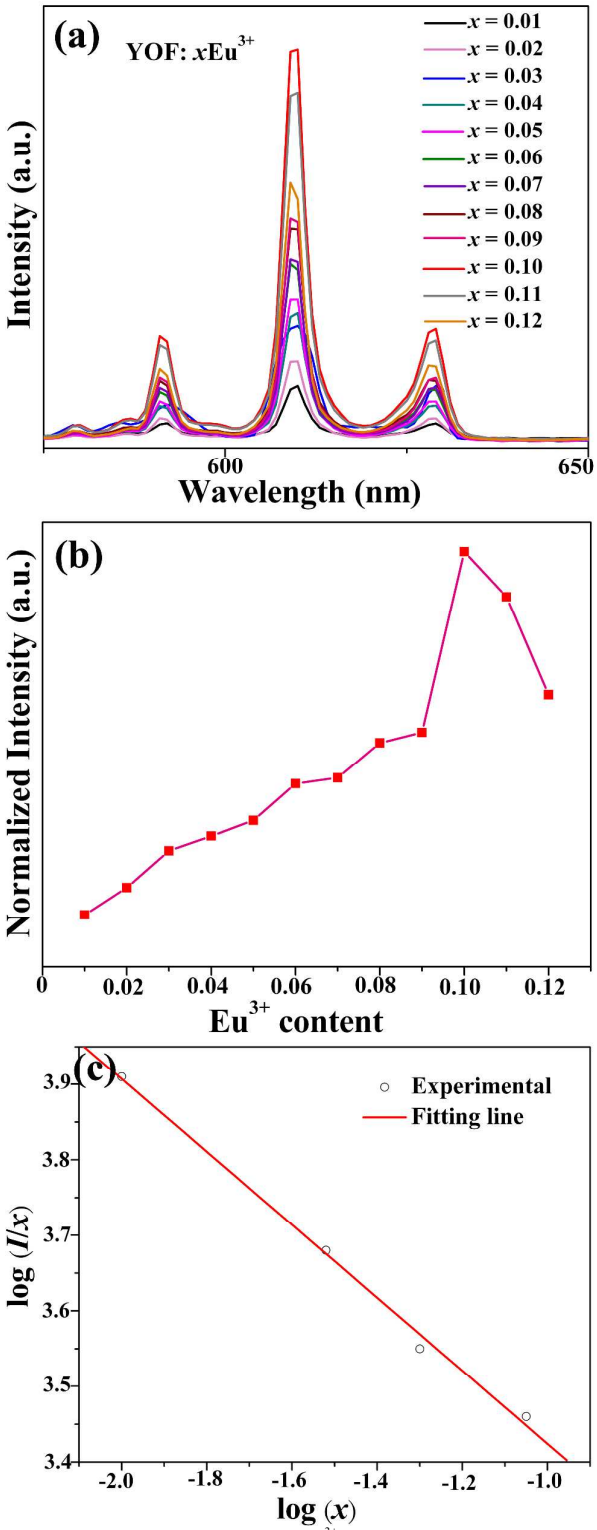

Fig.4 (a) Emission spectra of YOF:$x$$Eu^{3+}$ (x = 0–0.12)samples under 244 nm excitation; (b) variation of emission intensity as a function of Eu^{3+} content for YOF:$x$$Eu^{3+}$ phosphors; (c) dependence of log(I/x) on log(x) in YOF:$x$$Eu^{3+}$ samples.

due to the exchange interaction or multipole–multipole interaction when the activators is in high concentration.[40] According to the

report of Van Uiter, the emission intensity (I) per activator can be estimated using the following equation [41,42]

$$I/x = k\left[1+\beta(x)^{\theta/3}\right]^{-1} \quad (1)$$

where I is the emission intensity of Eu^{3+}, x is the Eu^{3+} doping concentration, k and β are constants for a given host under the same excitation condition, $\theta = 3$ stands for the energy transfer among the nearest neighbor ions, while $\theta = 6$, 8, and 10 represent the dipole–dipole, dipole–quadrupole, and quadrupole–quadrupole interactions, respectively. By taking the logarithm of eqn (1), the $\log(I/x)$ was plotted as a function of $\log(x)$ with a slope of $(-\theta/3)$ and was presented in Fig. 4c. The slope of fitted line was calculated to be –0.483 and thus, the θ was determined to be 1.449 indicating that the nearest neighbor ions is responsible for the concentration quenching of the Eu^{3+} ions. In addition, when Eu^{3+} doping concentration is higher than the critical concentration, the Eu^{3+} may form the ion pair, which leads to concentration quenching of the Eu^{3+} ions.[43–45]

The room temperature PL spectra of YOF:0.1Eu^{3+} samples with different doping concentration of Gd^{3+} ions under 244 nm excitation are shown in Fig. 5. It can be seen that the peak location and profile of the emission spectra of samples after Gd^{3+} ions doping are basically identical with those Gd–free sample, suggesting that the added Gd^{3+} ions would not influence the luminescent characteristics of YOF:Eu^{3+}. However, the PL intensities drastically changed with increasing Gd^{3+} doping concentration. The luminescence intensities distinctly increased when the concentration of Gd^{3+} ions increased from 0 to 0.35 mmol, but subsequently decreased with further increasing doping concentration. The strongest PL intensity was observed in the sample with a Gd^{3+} concentration of 0.35 mmol and the luminescence intensity were enhanced by 31 times than that of the Gd^{3+} free sample. The inset of Fig. 5 depicts the variation of the emission intensity as a function of doped Eu^{3+} content. It is generally accepted that luminescent property of phosphors is critically depend on the crystal structure and crystal field of the surroundings around Ln^{3+} ions.[33,35] To this end, we investigated the crystal field and crystal phase of $Y_xGd_{0.9-x}OF$:0.1Eu^{3+} crystals. As shown in Fig. S2 (ESI), the XRD patterns of the $Y_xGd_{0.9-x}OF$:0.1Eu^{3+} (x = 0–0.5) samples can be indexed to hexagonal and rhombohedral YOF, respectively. For hexagonal YOF (x = 0–0.2), when the Y^{3+} ions are substituted by the larger radius Gd^{3+} ions, the calculated lattice parameters tend to increase, indicating the expansion of host lattice dimension (Table S1, ESI). Based on the quantum selection rules, the intra 4f electronic transitions of Ln^{3+} ions strongly depend on their local crystal field. Thus, the substitution of Y^{3+} by Gd^{3+} ion would destroy the local crystal field around the Eu^{3+} ions, which can then expectedly enhance the radiative transition rate and their luminescence intensity.[21,46] For

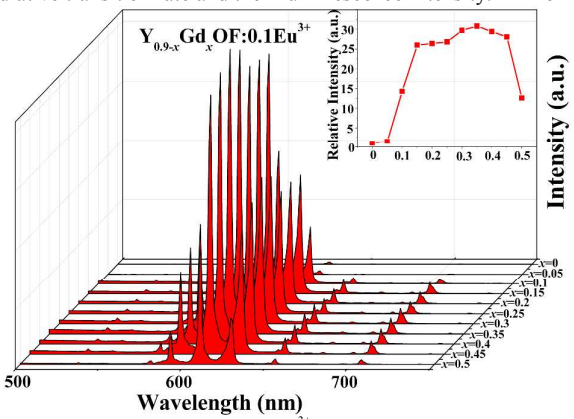

Fig.5 PL spectra of: $Y_{0.9-x}Gd_xOF$:0.1Eu^{3+} with different x values.

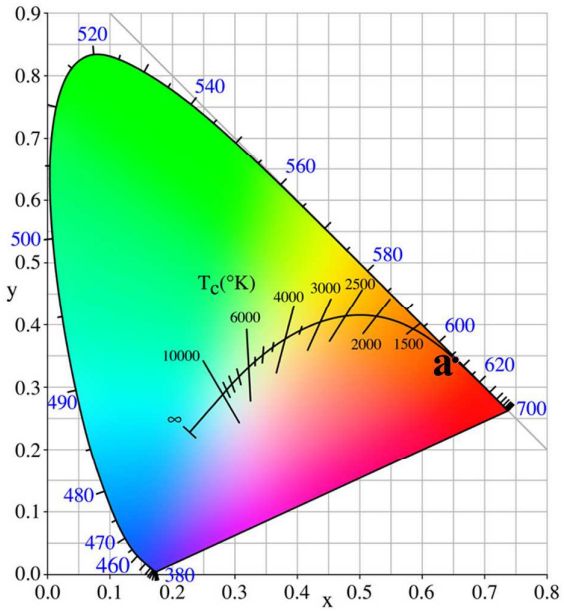

Fig.6 The CIE coordinate diagram for representative $Y_{0.55}Gd_{0.35}OF$:0.1Eu^{3+} phosphor under 244 nm excitation.

rhombohedral YOF (x = 0.25–0.5), the PL intensities enhance with increasing of Gd^{3+} concentration until x = 0.35, due to the destruction of local crystal field of Eu^{3+} ions. However, when the Gd^{3+} concentration exceeds the optimal value, luminescence intensity of the Eu^{3+} becomes weak, which means that concentration quenching effect of Gd^{3+} ion exists. It leads to the assumption that the Gd^{3+} ion induces significant distortion to the lattice, which affects the spatial distribution of lanthanide ions and induces concentration quenching, thus reduce the emission intensity. This phenomenon of initial enhancement and subsequent decrease of the emission intensity have also been observed in Li^{+}, Mo^{3+}, and Fe^{3+} doped crystals.[22,35,47] In addition, we first observed that the fluorescence performance of rhombohedral YOF is superior to that of hexagonal YOF.

The Commission Internationale de l'Eclairage (CIE) study has been performed on $Y_{0.9-x}Gd_xOF$:0.1Eu^{3+} samples. As a representative example, the CIE coordinate of synthesized $Y_{0.55}Gd_{0.35}$ OF:0.1Eu^{3+} sample is determined as (0.655, 0.344), located in the red region (point a in Fig. 6) with a correlated color temperature (CCT) of 2798 K. Detailed analysis of CIE coordinates and CCT of other samples are given in Table S2 (ESI†). This merit of highly enhanced emission males this material potential applications in the LEDs, and color display.

4. Conclusion

In summary, undoped and Eu^{3+} doped YOF and $Y_{1-x}Gd_xOF$ crystals were synthesized via a facile urea based homogeneous precipitation method followed by a heat treatment. The crystal phase transition, and morphology transformation of the samples can be first observed by Gd^{3+} doping. The luminescence properties and the quenching concentration of Eu^{3+} doped YOF samples were investigated upon UV excitation. More importantly, after doping Gd^{3+} ions, luminescence intensity of the sample enhanced by 31 times, which may due to modification of the crystal field and crystal phase of YOF. The prepared material may be a potential red phosphor material in LEDS.

Acknowledgements

This work was financially supported by the Mineral and Ore Resources Comprehensive Utilization of Advanced Technology Popularization and Practical Research (MORCUATPPR) funded by China Geological Survey (Grant No. 12120113088300).

Notes and references

1 H. Daicho, T. Iwasaki, Y. Maeno, Y. Shinomiya, *Nat. Commun.*, 2012, **3**, 1132.
2 C. K. Huang, Y. X. Ou, Y. Q. Bie, Q. Zhao and D. P. Yu, *Appl. Phys. Lett.*, 2011, **98**, 263104.
3 Q. Zhou, Y. Y. Zhou, Y. Liu, L. J. Luo, Z. L. Wang, J. H. Peng, J. Yan and M. M. Wu, *J. Mater. Chem. C,* 2015, **3**, 3055.
4 L. Agazzi, E. H. Bernhardi, K. Wörhoff, and M. Pollnau, *Appl. Phys. Lett.*, 2012, **100**, 011109.
5 Y. S. Liu, S. Y. Zhou, D. T. Tu, Z. Chen, M. D. Huang, H. M. Zhu, E. Ma, and X. Y. Chen, *J. Am. Chem. Soc.*, 2012, **134**, 15083.
6 J. Zhou, Q. Liu, W. Feng, Y. Sun, and F. Y. Li, *Chem. Rev.*, 2015, **115** , 395.
7 F. Wang, Y. Han, C. S. Lim, Y. H. Lu, J. Wang, J. Xu, H. Y. Chen, C. Zhang, M. H. Hong, and X. G. Liu, *Nature*, 2010, **463**, 1061.
8 M. Yang, X. D. Zhao, Y. Ji, F. Y. Liu, W. Liu, J. Y. Sun, and X. Y. Liu, *New J. Chem.*, 2014, **38**, 4249.
9 Y. Wang, S. L. Gai, N. Niu, F. He and P. P. Yang, *Phys. Chem. Chem. Phys.,* 2013, **15**, 16795.
10 G. P. Dong, B. B. Chen, X. D. Xiao, G. Q. Chai, Q. M. Liang, M. Y. Peng and J. R. Qiu, *Nanoscale*, 2012, **4**, 4658.
11 Z. H Xu, S. S. Bian, T. Liu, L. M. Wang, Y. Gao, H. Z. Lian and J. Lin, *RSC Adv.*, 2012, **2**, 11067.
12 Y. Gao, M. M. Fan, Q. H. Fang and W. Hana, *New J. Chem.,* 2013, **37**, 670.
13 S. Mourdikoudis, and L. M. L. Marzán, *Chem. Mater.*, 2013, **25**, 1465.
14 C. C. Yang, Y. H. Yu, B. Linden, J. C. S. Wu, and G. Mul, *J. Am. Chem. Soc.*, 2010, **132**, 8398.
15 X. M. Li, R. Wang, F. Zhang, and D. Y. Zhao, *Nano Lett.*, 2014, **14**, 3634.
16 F. Vetrone, R. Naccache, V. Mahalingam, C. G. Morgan, and J. A. Capobianco, *Adv. Funct. Mater.*, 2009, **19**, 2924.
17 W. Lü, W. Z. Lv, Q. Zhao, M. M. Jiao, B. Q. Shao and H. P. You, *J. Mater. Chem. C*, 2015, 3, 2334.
18 X. Feng, D. C. Sayle, Z. L. Wang, M. S. Paras, B. Santora, A. C. Sutorik, T. X. T. Sayle, Y. Yang, Y. Ding, X. Wang and Y. S. Her, *Science*, 2006, 312, 1504**.**
19 Q. Zhao, W. Lü, N. Guo, Y. C. Jia, W. Z. Lv, B. Q. Shao, M. M. Jiao and H. P. You, *Dalton Trans.*, 2013, 42, 6902.
20 B. P. Singh, A. K. Parchur, R. S. Ningthoujam, A. A. Ansari,d P. Singha and S. B. Raib, *Dalton Trans.*, 2014, **43**, 4779.
21 N. Niu, F. He, S. l. Gai, C. X. Li, X. Zhang, S. H. Huang and P. P. Yang, *J. Mater. Chem.*, 2012, **22**, 21613.
22 P. Ramasamy, P. Chandra, S. W. Rhee and J. Kim, *Nanoscale*, 2013, **5**, 8711.
23 L. Tao, W. Xu, Y. S. Zhu, L. Xu, H. C. Zhu, Y. X. Liu, S. Xu, P. W. Zhou and H. W. Song, *J. Mater. Chem. C*, 2014, **2**, 4186.
24 M. M. Shang, G. G. Li, X. J. Kang, D. M. Yang, D. L. Geng, C. Peng, Z. Y. Cheng, H. Z. Lian and J. Lin, *Dalton Trans.*, 2012, **41**, 5571.
25 Y. Zhang, X. J. Li, X. J. Kang, Z. Y. Hou and J. Lin, *Phys. Chem. Chem. Phys.,* 2014, **16**, 10779.
26 Z. H. Lia, L. Z. Zheng, L. N. Zhang, L. Y. Xiong, *J. Lumin.*, 2007, **126**, 481.
27 T. Grzyb, M. Wecławiak, J. Rozowska, S. Lis, *J. Alloys Comp.*, 2013, **576**, 345.
28 R. Q. Li, L. L. Li, W. W. Zi, J. J. Zhang, L. Liu, L. H. Zou and S. C. Gan, *New J. Chem.*, 2015, **39**, 115.
29 Y. Zhang, X. J. Li, D. L. Geng, M. M. Shang, H. Z. Lian, Z. Y. Cheng and J. Lin, *CrystEngComm*, 2014, 16, 2196.
30 Q. Ju, D. T. Tu, Y. S. Liu, R. F. Li, H. M. Zhu, J. C. Chen, Z. Chen, M. D. Huang, and X. Y. Chen, *J. Am. Chem.Soc.*, 2012, **134**, 1323.
31 S. J. Zeng, M. K. Tsang, C. F. Chan, K. L. Wong, B. Feid and J. H. Hao, *Nanoscale*, 2012, **4**, 5118.
32 X. F. Wang, Y. Y. Bu, Y. Xiao, C. X. Kan, Di Lu and X. H. Yan, *J. Mater. Chem. C*, 2013, **1**, 3158.
33 C. Liang, Z. Y. Wang, Y. Y. Zhang, W. K. Duan, W. Y. Yue, Y. Ding and W. Wei, *CrystEngComm*, 2014, **16**, 4963.
34 L. Rao, W. Lu, T. M. Zeng, Z. G. Yi, H. B. Wang, H. R. Liu and S. J. Zeng, *J. Mater. Chem. B*, 2014, **2**, 6527.
35 D. G. Yin, C. C. Wang, J. Ouyang, K. L. Song, B. Liu, X. Z. Cao, L. Zhang, Y. L. Han, X. Long and M. H. Wu, *Dalton Trans.*, 2014, **43**, 12037.
36 R. Q. Li, W. W. Zi, L. L. Li, L. Liu, J. J. Zhang, L. H. Zou, and S. C. Gan, *J. Alloys Comp.*, 2014, **617**, 498.
37 Y. Zhang, D. L. Geng, X. J. Kang, M. M. Shang, Y. Wu, X. J. Li, H. Z. Lian, Z. Y. Cheng, and J. Lin, *Inorg. Chem.*, 2013, **52**, 12986.
38 R. Krishnan and J. Thirumalai, *New J. Chem.,* 2014, 38, 3480.
39 Maheshwary, B. P. Singh, J. Singh and R. A. Singh, *RSC Adv.*, 2014, **4**, 32605.
40 D. L. Dexter, *J. Chem. Phys.*, 1953, **21**, 836.
41 L. G. V. Uitertm, *J. Lumin.*, 1971, **4**, 1.
42 M. M. Jiao, Y. C. Jia, W. Lü, W. Z. Lv, Q. Zhao, B. Q. Shao and H. P. You, *J. Mater. Chem. C*, 2014, **2**, 90.
43 A. Kumar, D. K. Rai, S. B. Rai, *Spectrochim. Acta A*, 2003, **59**, 917.
44 C. Jiang, W. S. Hu, and Q. J. Zeng, *IEEE J Quantum Elect*, 2003, **39**, 1266.
45 A. Patraa, G. A. Bakerb, S. N. Baker, *J. Lumin.*, 2005, **111**, 105.
46 S. X. Yan, J. H. Zhang, X. Zhang, S. Z. Lu, X. G. Ren, Z. G. Nie, and X. J. Wang, *J. Phys. Chem. C*, 2007, **111**, 13256.
47 A. K. Singh, S. K. Singh and S. B. Rai, *RSC Adv.*, 2014, **4**, 27039.